A Continuous-Wave Hybrid AlGaInAs–Silicon Evanescent Laser

Alexander W. Fang, *Student Member, IEEE*, Hyundai Park, *Student Member, IEEE*, Richard Jones, *Member, IEEE*, Oded Cohen, Mario J. Paniccia, *Senior Member, IEEE*, and John E. Bowers, *Fellow, IEEE*

***Abstract*—We report a novel laser architecture, the hybrid silicon evanescent laser (SEL), that utilizes offset AlGaInAs quantum wells (QWs) bonded to a silicon waveguide. The silicon waveguide is fabricated on a silicon-on-insulator wafer using a complimentary metal–oxide–semiconductor-compatible process, and is subsequently bonded with the AlGaInAs QW structure using low temperature O_2 plasma-assisted wafer bonding. The optical mode in the SEL is predominantly confined in the passive silicon waveguide and evanescently couples into the III–V active region providing optical gain. The SEL lases continuous wave (CW) at 1568 nm with a threshold of 23 mW. The maximum temperature for CW operation is 60 °C. The maximum single-sided fiber-coupled CW output power at room temperature is 4.5 mW.**

***Index Terms*—Complimentary metal–oxide–semiconductor, semiconductor lasers, silicon-on-insulator (SOI) technology.**

I. Introduction

SILICON is an attractive material for a silicon photonics platform because of its transparency at the communication wavelengths of 1.3 and 1.5 μm and because of its pervasiveness in the integrated electronics industry. Silicon's inefficient light generation has been the major hindrance for the realization of an electrically pumped laser on silicon, a key element for photonic integrated circuits. This has been addressed in the form of a Raman laser [1], [2] and material engineered light-emitting diode structures [3], [4] aimed at increasing light emission. We report here an approach that utilizes AlGaInAs quantum wells (QWs) bonded to silicon rib waveguides. The optical mode is predominantly in the silicon region with an evanescent tail overlapping into the offset quantum-well region. We recently reported a pulsed silicon evanescent laser (SEL) operating at 20 °C[5]. We report here a continuous-wave (CW) SEL operating at a maximum temperature of 60 °C. At 20 °C, the devices lase with a threshold of 23 mW and maximum fiber-coupled output of 4.5 mW. The confinement factor in the active region and device length was increased in the CW device to above 4.1% and 800 μm, respectively, from 3.6% and 600 μm in previous pulsed devices in order to increase gain and reduce effective mirror losses.

Manuscript received January 18, 2006; revised February 27, 2006. This work was supported by Jag Shah, by the Defense Advanced Research Projects Agency (DARPA), and by Intel Corp.

A. W. Fang, H. Park, and J. E. Bowers are with the Department of Electrical and Computer Engineering, University of California Santa Barbara, Santa Barbara, CA 93106 USA (e-mail: awfang@ece.ucsb.edu).

R. Jones and M. J. Paniccia are with the Photonics Technology Laboratory, Intel Corporation, Santa Clara, CA 95054 USA.

O. Cohen is with the Photonics Technology Laboratory, Intel Corporation, Jerusalem 91031, Israel.

Digital Object Identifier 10.1109/LPT.2006.874690

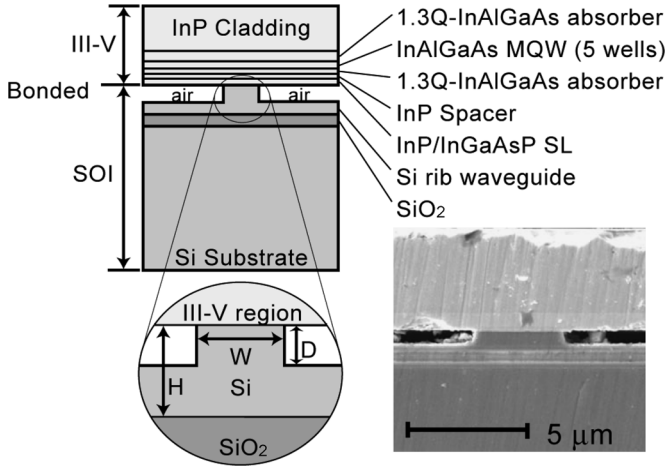

Fig. 1. Device structure cross section and cross section SEM image (inset).

II. Device Structure and Fabrication

The device structure is shown in Fig. 1. The device is divided into two regions: the silicon-on-insulator (SOI) passive-waveguide structure and the III–V active region that provides the optical gain. The SOI structure consists of a Si substrate, a 1-μm-thick SiO_2 lower cladding layer, and a Si rib waveguide with a height (H) and rib-etch depth (D) of 0.7 and 0.6 μm, respectively. The waveguide width (W) is varied from 1 to 5 μm. The III–V region consists of a two-period InP/1.1-μm InGaAsP superlattice (SL), a 110-nm-thick InP spacer, a 50-nm-thick unstrained 1.3-μm AlGaInAs separated confinement heterostructure (SCH) layer, strain-compensated AlGaInAs QWs, a 500-nm-thick unstrained 1.3-μm AlGaInAs SCH layer, and an InP upper cladding layer. The SL region employs 7.5-nm-thick alternating layers of InP–InGaAsP to inhibit the propagation of defects from the bonded interface to the QW region [6].

Five 7-nm-thick AlGaInAs QWs with compressive strain (0.85%) and 10-nm-thick AlGaInAs barriers with tensile strain (-0.55%) are used. The barrier layers have a bandgap corresponding to a wavelength of 1.3 μm.

The silicon rib waveguide is fabricated on the (100) surface of a lightly p-doped (doping concentration $< 2 \times 10^{15}$ cm^{-3}) SOI substrate by standard photolithography and reactive ion etching (RIE) plasma of Cl_2–HBr–Ar. A thin layer of SiO_2 was used as a hard mask. The SOI wafer and III–V epitaxial wafer are

treated by buffered HF and NH_4OH, respectively, after a thorough cleaning procedure using acetone, isopropanol, and deionized water. The two samples are bonded together via oxygen plasma assisted bonding [7]. After a low temperature anneal (300 °C), the InP substrate is removed with HCl. The devices are diced, the facets are polished, and the devices are characterized. Finally, the facets are coated with a broadband dielectric HR coating (∼80%) consisting of three periods of SiO_2–Ta_2O_5 and characterized again. The final device length after dicing and polishing is 800 μm. The bonded layer is continuous across the entire sample and is robust enough to stand up to dicing and polishing of the facets. The inset in Fig. 1 shows a scanning electron microscope (SEM) image of the fabricated device cross section. The particles on the facet surface are due to the polishing process.

The thermal expansion coefficient mismatch between Si $(2.6 \times 10^{-6}\ \mathrm{K}^{-1})$ and InP $(4.8 \times 10^{-6}\ \mathrm{K}^{-1})$ can introduce cracks in the III–V layers when bonding temperatures above 300 °C are used. Low temperature oxide mediated bonding was utilized to avoid these surface nonuniformities typically seen in direct wafer bonding conducted at 600 °C. The oxygen plasma treatment generates a thin oxide layer (<5 nm) whose surface is very smooth and highly chemically reactive [7]. As a result, this bonding process creates a thin oxide layer at the bonded interface; this does not significantly alter the optical mode because it is so thin and transparent at 1.55 μm.

III. Experiment and Results

The device is optically pumped perpendicular to the laser by a 1250-nm wavelength fiber. The light from the pump laser is focused by a cylindrical lens illuminating a 12 by 916 μm rectangular spot incident on the device through the top InP cladding layer. For the purpose of comparison, the incident pump power reaching the device was determined by measuring the reflected pump power and calculating the overlap of the pump beam with the laser mode. The power reflectivity from the bonded wafer at 1250 nm was measured to be 40%, and the laser mode was calculated by the length of the cavity multiplied by the computed mode widths of 9.36, 4.98, 4.38, 4.48, 5.18, and 5.18 μm for waveguide widths of 1, 1.5, 2.5, 3, 4, and 5 μm, respectively. The laser output is collected with a multimode fiber from the waveguide and subsequently characterized using a spectrum analyzer or photodetector. The fiber coupling efficiency is experimentally measured to be approximately −5.3 and −6.3 dB for 1- and 3-μm-wide devices, respectively, and can be assumed to be at least −5 dB. The TE/TM near-field images of the output mode are recorded on an IR camera through a polarizing beam splitter and an 80x lens at the opposite waveguide facet.

Figs. 2 and 3 show the laser output power as a function of pump power and temperature for two different waveguide widths of 4 and 1 μm. In Fig. 2, a 4-μm-wide device is operating with a threshold pump power of 23 mW with a fiber-coupled maximum output power of 4.5 mW and a slope efficiency of 3% at 20 °C. The total maximum output power taking into account the light from both facets and the coupling losses of 5 dB is approximately 28 mW and the corresponding slope efficiency is 16%. The threshold increases from 23 to 105 mW between

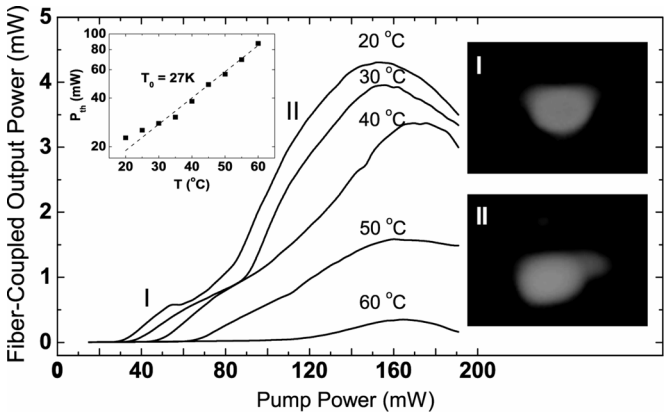

Fig. 2. LL curves and mode profiles for 800-μm-long 4-μm-wide device (inset) threshold versus temperature.

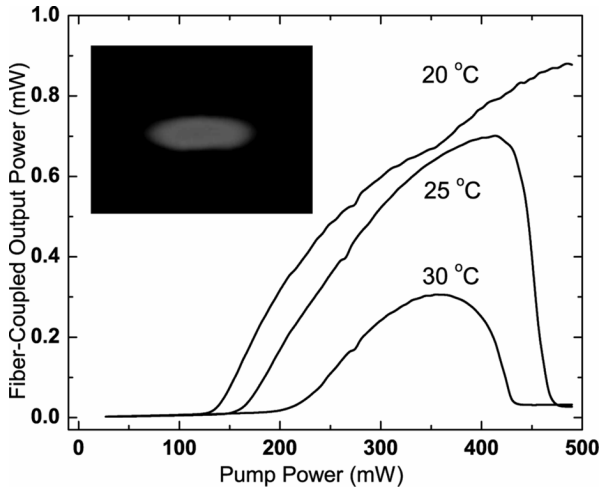

Fig. 3. LL curves and mode profile for 800-μm-long 1-μm-wide device.

20 °C and 60 °C and the structure exhibits a temperature coefficient (T_0) of 27 K. The kinks in the LL curves are due to the multimode lasing with wide waveguide dimension. It is clearly shown from two different mode profiles in Fig. 2 that higher modes are superimposed with a fundamental mode at the region II of the LL curve while only a fundamental mode is lasing at the region I. Fig. 3 shows LL curves of a 1-μm-wide device with a threshold of 120 mW and a slope efficiency of 0.5% at 20 °C. Since this waveguide width is narrower, the fundamental mode is lasing without other higher order modes up to 0.6 mW. This device demonstrates a maximum fiber-coupled output power of 0.9 mW. The total maximum output power including the output from both facets and coupling losses is approximately of 5 mW with a slope efficiency of 2.8%.

In Fig. 4, the threshold pump power dependence on waveguide width is shown for different temperatures. The wider stripe lasers have lower threshold pump power than narrower devices, since the wider devices have a lower modal overlap with device sidewalls and greater overlap in the silicon region over the III–V region. This results in lower scattering losses and lower overall propagation losses.

Fig. 5 shows the lasing spectrum of a 4-μm-wide device at two pump powers operating at 25 °C. The optical spectrum consists of the expected Fabry–Pérot response for the 800-μm-long

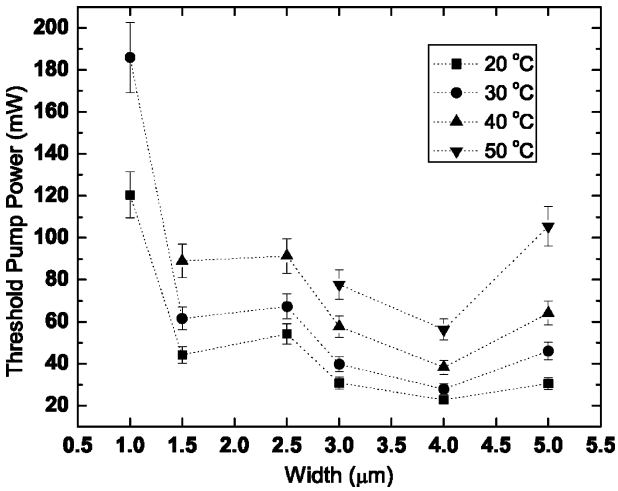

Fig. 4. Threshold pump power with different waveguide widths for 800-μm length.

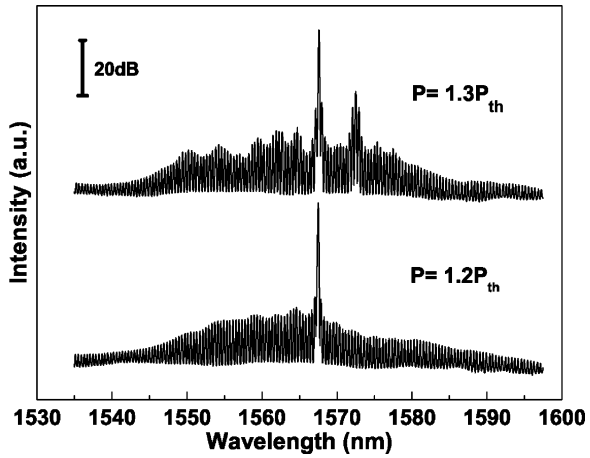

Fig. 5. Lasing spectra of a 4-μm-wide and 800-μm-long device.

cavity, with a group index of 3.68. The calculated group index from simulations is 3.77.

Sixty devices (ten devices at each of six widths) were characterized. Forty-seven of the sixty devices are lasing with a variation of threshold power for each waveguide width of less than $\pm$9%. The yield of the four wider widths is 98%, but the yield is lower for the narrower stripe widths due to damage during polishing.

The modal loss for the 4-μm-wide devices was measured experimentally to be $\sim$20 cm^{-1} by fabricating a second set of devices with lengths of 700 μm. The modal loss measurement was confirmed by taking Hakki–Paoli measurements in the long wavelength limit. The 700-μm HR-coated devices had a maximum output power of 2.7 mW at 20 °C and operated up to 60 °C for wider devices. They showed similar high yield, low device-to-device variation, and threshold versus waveguide width behavior to that of the 800-μm-long devices.

IV. Conclusion

We present here an optically pumped SEL operating CW at 1568 nm up to 60 °C. It has a maximum fiber-coupled output power of 4.5 mW with a threshold pump power of 23 mW. The laser utilizes low temperature oxide mediated bonding of offset AlGaInAs QWs to a silicon rib waveguide to achieve optical gain. The process provides high yield and low device-to-device performance variation. This structure can be extended to electrically pumped devices, such as lasers, amplifiers, and modulators, through the doping of III–V layers and minor backside processing.

Acknowledgment

The authors would like thank K. Callegari and G. Zeng for sample prep and C. S. Suh for taking SEM images.

References

[1] H. Rong, R. Jones, A. Liu, O. Cohen, D. Hak, A. Fang, and M. Paniccia, "A continuous-wave Raman silicon laser," *Nature*, vol. 433, pp. 725–728, 2005.

[2] O. Boyraz and B. Jalali, "Demonstration of a silicon Raman laser," *Opt. Express*, vol. 12–21, pp. 5269–5273, 2004.

[3] W. L. Ng, M. A. Lourenco, R. M. Gwilliam, S. Ledaim, G. Shao, and K. P. Homewood, "An efficient room-temperature silicon-based light-emitting diode," *Nature*, vol. 410, pp. 192–194, 2001.

[4] S. G. Cloutier, P. A. Kossyrev, and J. Xu, "Optical gain and stimulated emission in periodic nanopatterned crystalline silicon," *Nature Materials*, vol. 4, pp. 887–891, 2005.

[5] H. Park, A. W. Fang, S. Kodama, and J. E. Bowers, "Hybrid silicon evanescent laser fabricated with a silicon waveguide and III-V offset quantum wells," *Opt. Express*, vol. 13, no. 23, pp. 9460–9464, 2005.

[6] A. Karim, K. A. Black, P. Abraham, D. Lofgreen, Y. J. Chiu, J. Piprek, and J. E. Bowers, "Superlattice barrier 1528-nm vertical-cavity laser with 85 °C continuous-wave operation," *IEEE Photon. Technol. Lett.*, vol. 12, no. 11, pp. 1438–1440, Nov. 2000.

[7] D. Pasquariello and K. Hjort, "Plasma-assisted InP-to-Si low temperature wafer bonding," *IEEE J. Sel. Topics Quantum Electron.*, vol. 8, no. 1, pp. 118–131, Jan./Feb. 2002.